Classification of Hyperspectral Agricultural Data with Spectral Matching Techniques

K. Staenz, J. Schwarz, L. Vernaccini, F. Vachon, and C. Nadeau
Canada Centre for Remote Sensing
588 Booth Street, Ottawa, Ontario, Canada K1A 0Y7
Phone: (613) 947-1250, Fax: (613) 947-1383, E-mail: karl.staenz@ccrs.nrcan.gc.ca

ABSTRACT

This paper describes three new statistical spectral matching techniques (correlation, normalized Chi-square, and normalized square error statistics) and their application to agriculture for field labelling purposes. The resulting classifications were compared with each other and against those retrieved with the spectral angle mapper, a widely used spectral matching technique. Hyperspectral 96-band *casi* data acquired over an agricultural site near Altona, Manitoba, Canada were used for this purpose. The results of the single-class approach indicate that the best overall performance was achieved with the correlation similarity measure and the modified spectral angle mapper (MSAM) with about 84% and 78 % correctly classified pixels, respectively. The average classification accuracy was significantly lower for the normalized Chi-square and the normalized square error statistics (SES_N) techniques. The multi-class approach produced slightly better results in most cases due to lower co-mission errors.

Keywords: Spectral matching, hyperspectral data, surface reflectance retrieval, agriculture, classification.

1. INTRODUCTION

Substantial progress has been made in the development of new hyperspectral classification procedures for various applications over the past decade. The effort led to target identification techniques such as binary encoding (Mazer et al., 1988; Jia and Richards, 1993), spectral unmixing (Adams et al., 1989; Boardman, 1993; Szeredi et al., 1999), and spectral matching (Kruse et al., 1993a; Van Der Meer and Bakker, 1997; Schwarz and Staenz, 1999). Other techniques, for example, include the N-dimensional Probability Density Function (NPDF) (Cetin et al., 1993) and neural networks (Brown and Rouin, 1992; Abuelgasim et al., 1996). In addition, various conventional classification techniques were adapted to process hyperspectral data using approaches such as the maximum likelihood technique (Lee and Landgrebe, 1993; Jia and Richards, 1994) and indicator kriging (Van der Meer, 1994). Many of the hyperspectral target identification procedures require a reduction of the spectral dimensionality prior to the actual classification (Landgrebe, 1997; Harsanyi and Chang, 1994; Boardman et al., 1995). Incorporating artificial intelligence techniques into hyperspectral classification procedures led to advances in the automation of identification of target materials (Kruse et al., 1993b; Goodenough et al., 1995).

In general, these procedures are computationally intensive and require considerable user interaction to produce satisfactory results. Although computationally fast, the spectral matching techniques, incorporating similarity measures to compare a prototype spectrum with a spectrum to be classified, require the user to set a threshold for acceptance/rejection of matching two spectra (Schwarz and Staenz, 1999). Another limitation with spectral matching, and with most other hyperspectral target identification procedures with the exception of spectral unmixing, is the classification of multiple target materials within a pixel (mixed pixel problem). However, due to the straightforward application of spectral matching and its processing speed, this procedure is appropriate when general information on target type distribution needs to be extracted quickly or before carrying out detailed analyses. Furthermore, spectral matching can assist in the detection of the purest pixels in a scene for a given target material and used as training area for other hyperspectral target identification procedures, for instance, as endmember in spectral unmixing. It also plays an important role in searching spectral libraries for specific target materials.

In this paper, the performance of three spectral matching techniques based on statistical approaches (correlation, square error statistics, Chi-square) were evaluated in an agricultural setting against the spectral angle mapper (SAM) (Kruse et al., 1993a). For this purpose, the spectral matching techniques were applied to hyperspectral data acquired with the Compact Airborne Spectrographic Imager (*casi*) for crop type identification. The performance analysis, including data preprocessing such as the retrieval of surface reflectance, was carried out on the Imaging Spectrometer Data Analysis System (ISDAS) (Staenz et al., 1998).

2. *DATA USED*

Hyperspectral data acquired with the *casi* sensor over an agricultural site near Altona, Manitoba, Canada on July 25, 1996 were used for this study. This data set provides a good test case for a comparison of the different spectral matching algorithms because of a variety of common crop types present in the scene in combination

with extensive ground reference information available from the test site. This site, which has no significant topographic relief, included cash crops, such as cereal grains (wheat, barley), canola, and beans. A typical field size is about 400 m by 800 m. Ground reference information relevant for this paper includes crop type, crop appearance (height, density), and crop condition (biomass, chlorophyll, plant water concentration). The data set was collected in 96 contiguous, 6.8 nm wide spectral bands, sampled at 5.8 nm intervals (Anger et al., 1996). In this data acquisition configuration, the swath consists of 304 pixels with a spatial resolution of 4 m across and 4 m along track at a flight altitude of about 2500 m above ground level. The wavelength range was set from 458 nm to 1000 nm.

3. DATA PROCESSING

The pre-processing of *casi* data included the removal of non-periodic banding noise, the most significant aircraft motion effect, surface reflectance retrieval, and post-processing of the retrieved surface reflectance spectra. The data pre-processing scheme relevant for surface reflectance retrieval is outlined in Figure 1.

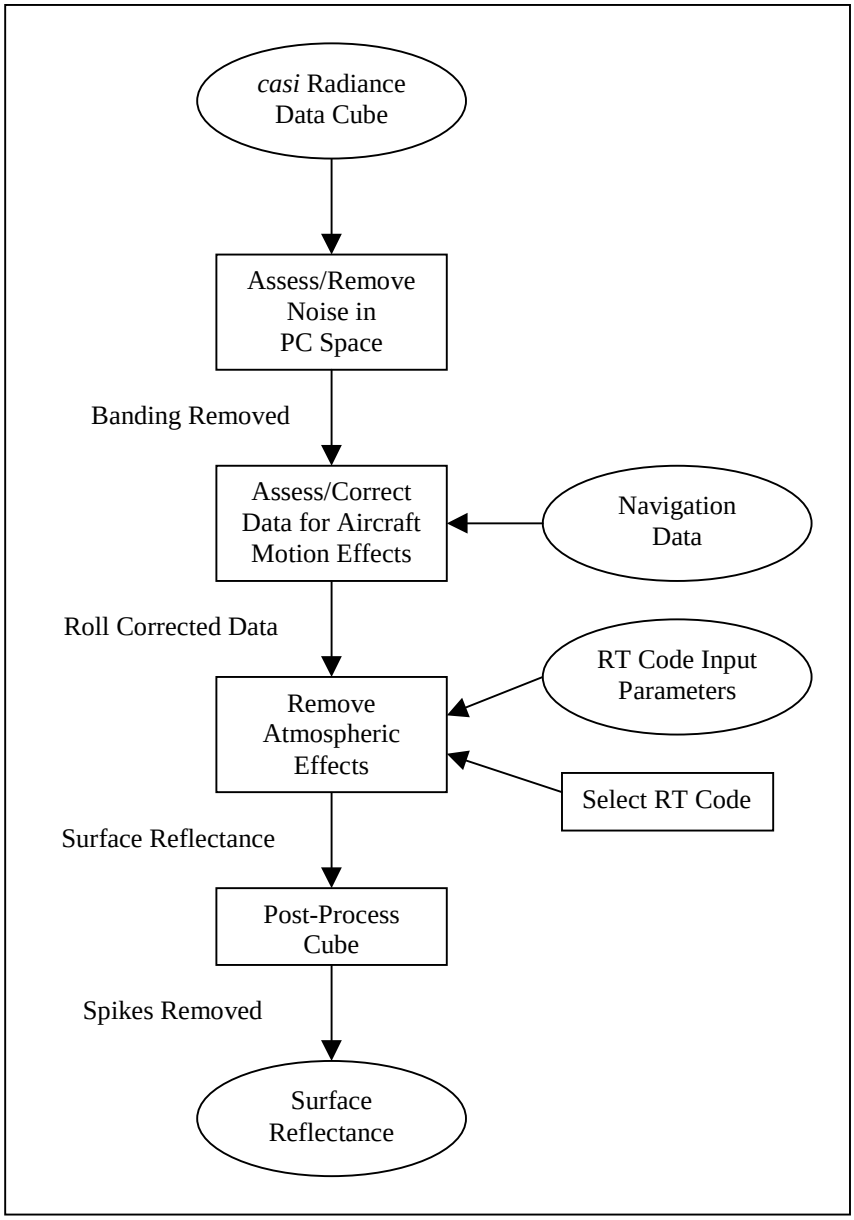

Figure 1: Data processing flow for the retrieval of surface reflectance (RT = Radiative Transfer).

3.1 Noise Removal

Temporally variable, non-periodic horizontal banding, which especially affects bands at the two extremes of the *casi* wavelength coverage, was removed in the principal component (PC) domain using the last 89 of 96 PC images. The average of each line per image for these 89 components was calculated and subsequently plotted against the line number. A Gaussian smoothing with a window of 15 lines was then applied to the data. This enabled the computation of a correction factor (gain) for each line to adjust the original mean values to the smoothed ones. The gain was calculated by dividing the smoothed values by the original line means. In a final step, the entire 96-PC image set was inversely transformed back to the spectral band domain.

3.2 Aircraft Motion Effect

In assessing the data quality, it was noted that significant aircraft motion effects exist in the *casi* imagery. In order to correct for the most significant aircraft motion effect, the roll was estimated using the navigation data to calculate lateral pixel shifts for each line. These shifts were then applied to the entire image cube on a line by line basis.

3.3 Surface Reflectance Retrieval

In the next processing steps, surface reflectances were computed from calibrated at-sensor radiance data, compensating for atmospheric absorption and scattering effects. The procedure is based on a look-up table (LUT) approach with tunable breakpoints as described in Staenz and Williams (1997), to reduce significantly the number of radiative transfer (RT) code runs. MODTRAN3 was used in forward mode to generate the radiance LUTs, one for each of a 5% and 60% flat reflectance spectrum. These LUTs were produced for five pixel locations equally spaced across the swath, including nadir and swath edges, and for single values of aerosol optical depth (horizontal visibility) and terrain elevation, and for a range of water vapour contents. The specification of these parameters and others required for input into the MODTRAN3 RT code are listed in Table 1. For the retrieval of the surface reflectance, the LUTs were adjusted only for the pixel position and water vapour content using a bi-linear interpolation routine (Press et al., 1992) since single values for the other LUT parameters were used for the entire cube. For this purpose, the water vapour content was estimated for each pixel in the scene with an iterative curve fitting technique (Staenz et al., 1997).

Table 1: Input Parameters for MODTRAN3 Code Runs

Atmospheric model	Mid-latitude summer
Aerosol model	Continental
Date of overflight	July 25, 1996
Solar zenith angle	31.3°
Solar azimuth angle	155.9°
Sensor zenith angle	Variable
Sensor azimuth angle	Variable
Terrain elevation above sea level	0.250 km
Sensor altitude above sea level	2.745 km
Water vapour content	Variable
Ozone column	as per model
CO_2 mixing ratio	as per model
Horizontal visibility	40 km

3.4 *Post-processing*

In a last step, band-to-band errors remaining in the 820 nm to 1000 nm range of the retrieved surface reflectance spectra resulting from inaccuracies in the atmospheric modelling and sensor calibration were removed using a Gaussian smoothing with an 80 nm window. A reflectance spectrum of canola is shown in comparison with non-smoothed data in Figure 2.

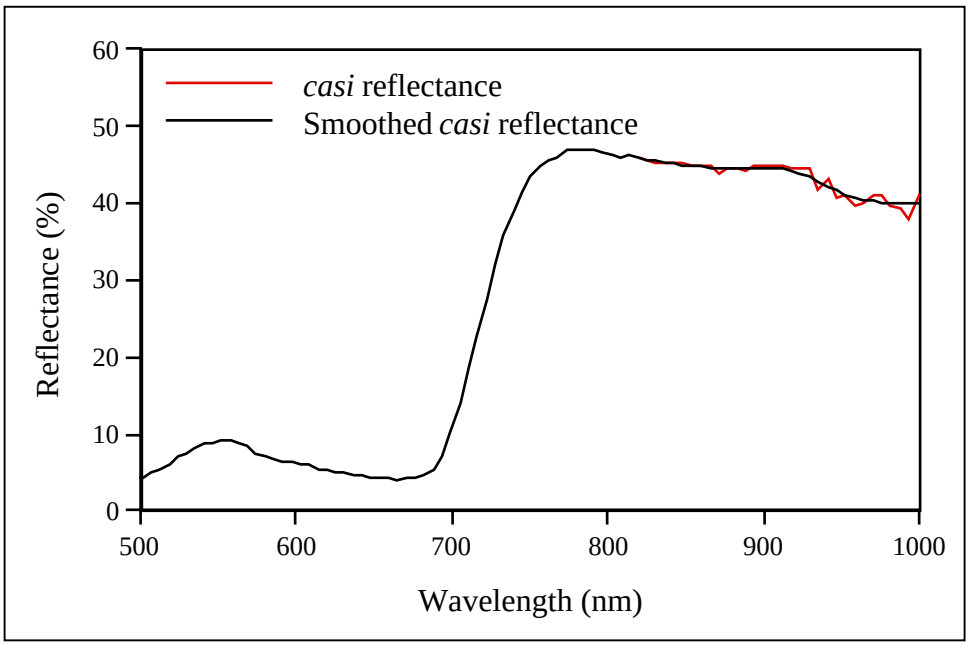

Figure 2: casi surface reflectance of canola. The casi spectrum was averaged over four adjacent pixels.

4. SPECTRAL MATCHING PROCEDURES

Each of the following techniques calculates a goodness of fit value (similarity measure) on a pixel basis between a reference spectrum and a spectrum to be matched (test spectrum). All the techniques have been implemented such that the resulting similarity values are between 0 and 1 where 1 indicates a perfect match.

- The correlation similarity measure C is based on the Pearson correlation coefficient (Snedecor and Cochran, 1967) and is expressed as the coefficient of determination as follows:

$$C = \left(\frac{M - n\bar{t}\bar{r}}{(n-1)\sigma_t \sigma_r} \right)^2 , \quad (1)$$

where

$$M = \sum_{b=1}^{n} t_b r_b , \quad (2)$$

r_b is the amplitude of the reference spectrum at band b, t_b is the amplitude of the spectrum to be matched at band b, $\bar{r}$ is the mean amplitude of the reference spectrum, $\bar{t}$ is the mean amplitude of the spectrum to be matched, σ_r is the standard deviation of the reference spectrum, σ_t is the standard deviation of the spectrum to be matched, and n is the number of bands.

- The Chi-square similarity measure X^2 is expressed as follows (Press et al., 1997):

$$X^2 = \sum_{b=1}^{n} \left(\frac{(t_b - r_b)^2}{r_b} \right). \quad (3)$$

In order to achieve similarity values between 0 and 1, the Chi-square is normalized as follows:

$$X_N^2 = 1 - \frac{X^2}{X_{\max}^2} \ . \quad (4)$$

- A third technique summarizes the deviations between two spectra by Square Error Statistics (SES) (Snedecor and Cochran, 1967). The similarity measure SES can then be expressed as follows:

$$SES = \sum_{b=1}^{n} \left(\frac{st_b - r_b}{\sigma_{r_b}} \right)^2 \text{ and } s = \sum_{b=1}^{n} r_b \Big/ \sum_{b=1}^{n} t_b \ , \quad (5)$$

where σ_{r_b} is the standard deviation in band b of the reference spectrum. The expression in equation (5) was normalized such that the similarity values lie between 0 and 1:

$$SES_N = 1 - \frac{SES}{SES_{\max}} . \quad (6)$$

- The similarity measure used as the baseline is the modified spectral angle mapper (MSAM) as introduced by Schwarz and Staenz, 1999. The similarity measure MSAM was modified from the spectral angle mapper (SAM) (Kruse et al., 1993a) as follows:

$$MSAM = 1 - \frac{2SAM}{\pi}, \quad (7)$$

where

$$SAM = \cos^{-1} \left(\frac{M}{\sqrt{\sum_{b=1}^{n} t_b^2 \sum_{b=1}^{n} r_b^2}} \right). \quad (8)$$

All the techniques are insensitive to gain factors (amplitude). However, if the scaling parameter s in equation (5) is set to 1, SES_N is dependent on the spectrum amplitude. In this case, the expression in the brackets of equation (5) is the square of the normalized Euclidean distance. The reference spectrum for a given target type (class) can be generated from a training area within the image cube to be classified or from a spectral library.

5. PERFORMANCE ANALYSIS

The spectral matching techniques were applied to the different target types in both single-class and multi-class modes. In single-class mode, a technique is applied to each class individually while in multi-class mode all classes are included sequentially during a single run of a specific technique. The classes analyzed consist of the following agricultural target types: wheat, barley, canola, and beans. The statistics (mean reference spectrum and standard deviation) for each individual class were generated from the training areas with a

minimum size of 286 pixels. The mean spectra of the training areas for the different classes are shown in Figure 3. In both classification modes, the classification results were achieved using the frequency histogram to set the threshold for the acceptance or refusal of a spectrum (Schwarz and Staenz, 1999). For instance, Figure 4 shows the distribution of the correlation measure for comparing the reference spectrum of barley against the entire scene. The cluster of values closest to unity represents predominantly canola spectra. Accordingly, the threshold is set at the local minimum situated between the barley and the previous cluster as indicated with an arrow in Figure 4.

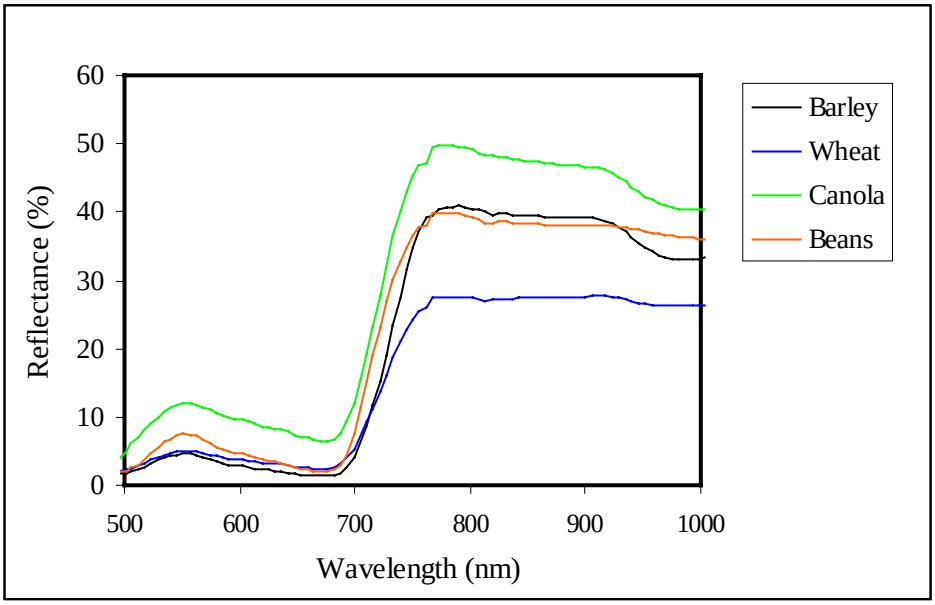

Figure 3: Mean reflectance spectra of training areas of the different classes. The spectra were produced from 486 pixels (barley), 770 pixels (wheat), 286 pixels (canola), and 986 pixels (beans).

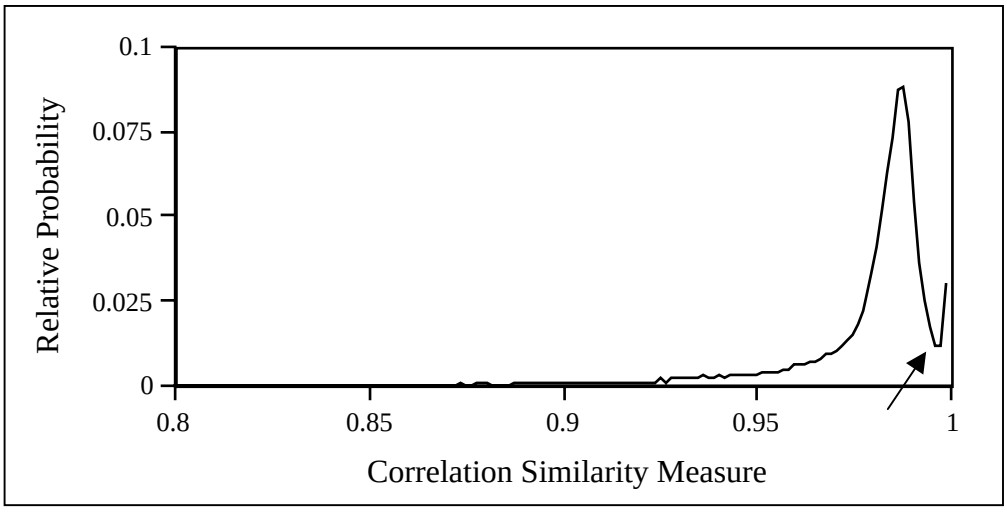

Figure 4: Threshold setting for the class barley using the frequency histogram which was generated with the correlation simularity measure. The arrow indicates the threshold selected.

The resulting classifications generated by using the different spectral matching techniques were compared with each other on a pixel-by-pixel basis. In order to determine the overall performance of the four matching techniques, the classified images were compared against a reference classification and omission/co-mission errors were calculated for each class. The reference classification was manually defined by examining spectra of individual border pixels to determine field boundaries. In our case, this simple technique was sufficient to generate a reference map since the field borders were clearly visible. Inclusions of soil patches and other non-crop materials within the fields were excluded from class membership.

6. RESULTS

Table 2 summarizes the classification results using the single-class approach. It can be seen that the correlation and the MSAM techniques classified on average 83.7 % and 77.5 % of the pixels in the scene correctly. The normalized Chi-square and SES_N techniques are next with 71.7 % and 67.9 %, respectively. The modified SAM shows on average the lowest co-mission error of about 7.6 %, followed by the SES_N with 8.6 %, the Chi-square with 10.2 % and the correlation with 11.4 %. Taking all three measures (correctly classified pixels, omission and co-mission error) into account, the correlation technique is the best performer followed by MSAM, normalized Chi-square and SES_N. Individual classification results indicate that the correlation technique performed significantly better for beans and wheat than the other techniques. Only slightly better results were achieved for beans with this similarity measure than with the MSAM. The larger co-mission errors for barley and wheat are due to the fact that some of the cloud shadow in some of the fields is spectrally very similar to barley or wheat and, therefore, cloud pixels were classified as one of these crop types. Canola was classified with a higher accuracy (over 89 %) than the other crop types. This is mainly due to the high plant density and lower within-field variation of this crop type causing a distinct spectral behaviour with less spectral variation than the other crop types (Figure 3). Due to the high plant density of canola, soil is less of a contributor to the pixel reflectance than, for example, row crops such as beans. There is no clear trend among the crop types with respect to the lowest classification accuracies. The accuracies for barley and beans are relatively low because their spectral behaviour is similar as shown in Figure 3. It should be noted that the results are dependent on the selection of the training areas and the threshold for the acceptance or rejection of a pixel. However, using the frequency histogram to select a threshold is a technique that adapts to changes in the training area set, while maintaining good classification performance. Table 3 shows the thresholds for the different similarity measures for the classification of the different crop types.

Table 2: Classification results of the different spectral matching techniques using the single-class approach (A = correct classified pixels; B = omission error; C = co-mission error; n = total number of reference pixels; nt = number of pixels in the training area).

Matching Technique	**Classification Type**	**%-Pixel Classified**				
		Barley (n=3979) (nt=468)	**Beans** (n=32464) (nt=986)	**Canola** (n=21840) (nt=268)	**Wheat** (n=26771) (nt=770)	**Average**
Correlation	A	75.99	76.68	97.39	84.86	83.73
	B	24.01	23.32	2.61	15.14	16.27
	C	12.29	9.02	4.27	19.81	11.35
Chi-square	A	54.79	67.05	89.95	75.10	71.72
	B	45.21	32.95	10.05	24.90	28.28
	C	12.56	3.62	3.87	20.78	10.21
SES_N	A	62.50	66.12	90.67	52.44	67.93
	B	37.50	33.88	9.33	47.56	32.07
	C	10.38	5.66	10.08	8.22	8.59
MSAM	A	73.85	67.57	97.68	71.01	77.54
	B	26.15	32.43	2.32	28.99	22.46
	C	10.63	2.66	3.49	13.64	7.61

Table 3: Threshold for acceptance or rejection of pixels by the similarity measures.

Crop Type	Correlation	SES_N	Norm. Chi-square	MSAM
Barley	99.75	99.90	99.60	97.50
Beans	99.75	99.91	99.10	97.80
Canola	99.60	99.75	96.30	97.10
Wheat	99.65	99.84	99.20	97.50

The same training areas and thresholds were used to run the multi-class approach. The classification results from this approach are listed in Table 4. It can be seen that the correctly classified pixels and the omission errors are basically the same as produced with the single-class approach. However, the co-mission errors are generally lower for the multi-class mode. This means that the multi-class approach produces better classification results. As an example, the multi-class results generated with the correlation and the MSAM techniques are shown in Figure 5.

Table 4: Classification results of the different spectral matching techniques using the multi-class approach (A = correct classified pixels; B = omission error; C = co-mission error; n = total number of reference pixels; nt = number of pixels in the training area).

Matching Technique	**Classification Type**	**%-Pixel Classified**				
		Barley (n=3979) (nt=468)	**Beans** (n=32464) (nt=986)	**Canola** (n=21840) (nt=268)	**Wheat** (n=26771) (nt=770)	**Average**
Correlation	A	75.95	76.56	97.07	83.15	83.18
	B	24.05	23.44	2.93	16.85	16.82
	C	12.19	7.51	3.71	14.81	9.56
Chi-square	A	54.79	66.90	89.95	75.10	71.69
	B	45.21	33.10	10.05	24.90	28.31
	C	9.93	2.80	3.68	20.78	9.30
SES_N	A	62.50	65.47	90.67	52.43	67.77
	B	37.50	34.53	9.33	47.57	32.23
	C	10.38	4.26	2.62	8.06	6.33
MSAM	A	73.84	67.47	97.68	70.82	77.45
	B	26.16	32.53	2.32	29.18	22.55
	C	10.63	1.89	3.50	10.06	6.52

7. CONCLUSIONS

Three new statistical spectral matching techniques, correlation, normalized Chi-square and normalized square error statistics, were applied to a 96-band *casi* data set for classification of agricultural targets. The spectral matching techniques were run in single-class and multi-class modes. The classifications were generated using the frequency histogram as a technique to set the threshold for the acceptance or rejection of a pixel spectrum. The resulting classifications were compared with each other and to those produced with the MSAM. The study shows that the spectral matching techniques can be used with reasonable accuracy for classification of agricultural targets. However, the various methods can produce different results. The following specific conclusions can be drawn:

- The correlation similarity measure performs as well or even better than the MSAM for some targets. An overall classification accuracy of about 84 % was achieved with the correlation technique while MSAM produced an average classification accuracy of 78 %.

- The average classification accuracies of 72 % and 68 % for the normalized Chi-square and SES_N similarity measures were significantly lower than for the other techniques.

- The best individual classification accuracies of over 97 % were achieved for canola using the correlation an MSAM measures. The lowest accuracies occur for wheat and barley using the SES_N and the normalized Chi-square similarity measures, respectively.

- The highest co-mission errors with up to 21 % occur for barley and wheat.

- With similar percentage of correctly classified pixels and omission errors, the multi-class approach produces slightly better classification results in most cases than the single classification scheme due to lower co-mission errors.

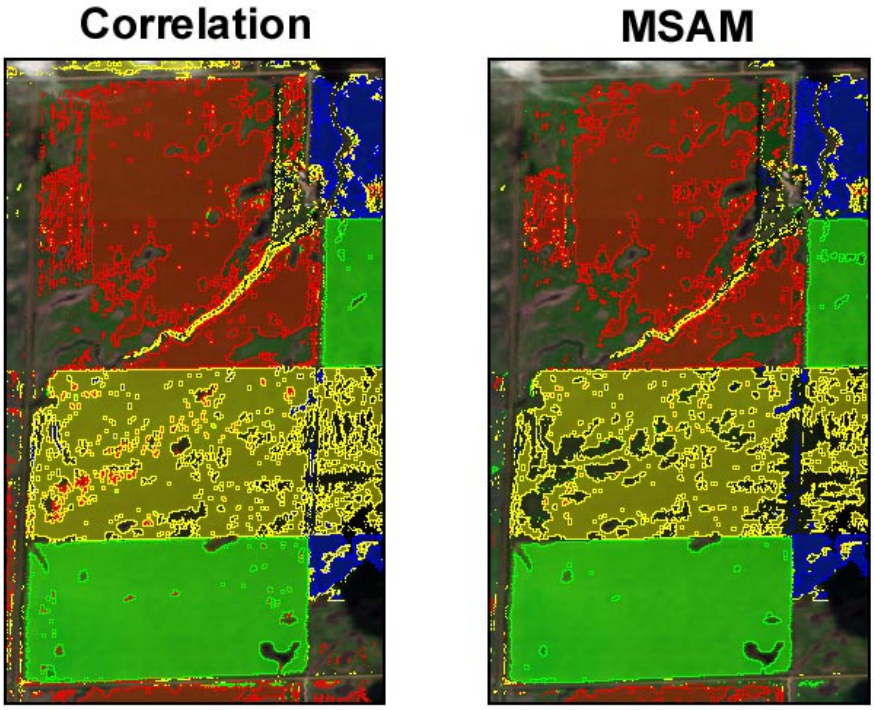

Figure 5: Multi-class results achieved with the correlation similarity measure and the Modified Spectral Angle Mapper (MSAM). The classes are barley (blue), beans (red), canola (green), and wheat (yellow).

8. ACKNOWLEDGEMENTS

The authors wish to thank J. Lévesque of MIR Télétédection for her technical assistance.

9. REFERENCES

Abuelgasim, A., S. Gopal, J.R. Irons, and A.H. Strahler, 1996, "Classification of ASAS Multiangle and Multispectral Measurements Using Artificial Neural Networks", Remote Sensing of Environment, 57:79-87.

Anger, C.D., S. Achal, T. Ivanco, S. Mah, R. Price, and J. Busler, 1996, "Extended Operational Capabilities of *casi*", Proceedings of the 2nd International Airborne Remote Sensing Conference, San Francisco, California, pp.124-133.

Adams, J.B., M.O. Smith, and A.R. Gillespie, 1989, "Simple Models for Complex Natural Surfaces: A Strategy for the Hyperspectral Era of Remote Sensing", Proceedings of the International Geoscience and Remote Sensing Symposium (IGARSS'89) and the 12th Canadian Symposium on Remote Sensing, Vancouver, British Columbia, Vol. 1, pp.16-21.

Boardman, J.W., 1993, "Automating Spectral Unmixing of AVIRIS Data Using Convex Geometry Concepts", Summaries of the 4th Annual JPL Airborne Geoscience Workshop, JPL Publication 93-26, Pasadena, California, Vol. 1, pp.11-14.

Boardman, J.W., F.A. Kruse, and R.O. Green, 1995, "Mapping Target Signatures Via Partial Unmixing of AVIRIS Data", Summaries of the Fifth Annual JPL Airborne Earth Science Workshop, JPL Publication 95-1, Pasadena, California, pp.23-26.

Brown, J.R., and E.D. Rouin, 1992, "Comparing Neural Network Classifiers and Feature Selection for Target Detection in Hyperspectral Imagery", Proceedings of the International SPIE Conference on Applications of Artificial Networks III, Vol. 1709, pp.167-173.

Cetin, H., T.A. Warner, and D.W. Levandowski, 1993, "Data Classification, Visualization, and Enhancement Using n-dimensional Probability Density Function (nPDF): AVIRIS, TIMS, TM, and Geophysical Application", Photogrammetric Enginnering and Remote Sensing, 59(12):1755-1764.

Goodenough, D.G., D. Charlebois, A.S. Bhogal, M.Heyd, S. Matwin, O. Niemann, and F. Portigal, 1995, "Knowledge-Based Imaging Spectrometer Analysis and GIS for Forestry", Proceedings of the International Geoscience and Remote Sensing Symposium (IGARSS'95), Florence, Italy, pp.464-476.

Harsanyi, J.C., and C.I. Chang, 1994, "Hyperspectral Image Classification and Dimensionality Reduction: An Orthogonal Subspace Projection Approach", IEEE Transactions on Geoscience and Remote Sensing, 32(4):779-785.

Jia, X., and J.A. Richards, 1993, "Binary Encoding of Imaging Spectrometer Data for Fast Spectral Matching and Classification", Remote Sensing of Environment, 43:47-53.

Jia, X., and J.A. Richards, 1994, "Efficient Maximum Likelihood Classification for Imaging Spectrometer Data Sets", IEEE Transactions on Geoscience and Remote Sensing, 32(2):274-281.

Kruse, F.A., A.B. Lefkoff, and J.W. Boardman, K.B. Heidebrecht, A.T. Shapiro, P.J. Barloon, and A.F.H. Goetz, 1993a, "The Spectral Image Processing System (SIPS) – Interactive Visualization and Analysis of Imaging Spectrometer Data", Remote Sensing of Environment, 44:145-163.

Kruse, F.A., A.B. Lefkoff, and J.B. Dietz, 1993b, "Expert System-Based Mineral Mapping in Northern Nevada Death Valley, California/Nevada, Using the Airborne Visible/Infrared Imaging Spectrometer (AVIRIS)", Remote Sensing of Environment, 44:309-336.

Landgrebe, D.A., 1997, "On Information Extraction Methods for Hyperspectral Data", Proceedings of the International Symposium for Spectral Sensing Research (ISSSR'97), San Diego, California, CD-ROM, 8 pages.

Lee, C., and D.A. Landgrebe, 1993, "Analyzing High-Dimensional Multispectral Data", IEEE Transactions on Geoscience and Remote Sensing, 31(4):792-800.

Mazer, A.S., M. Martin, M. Lee, and J.E. Solomon, 1988, "Image Processing Software for Imaging Spectrometer Data Analysis", Remote Sensing of Environment, 24(1):201-210.

Press, W.H., S.A. Teukolsky, W.T. Vetterling, and B.P. Flannery, 1992, Numerical Recipes in C, Cambridge University Press, Cambridge, England, pp.123-125.

Schwarz, J., and K. Staenz, 1999, “Adaptive Threshold for Spectral Matching of Hyperspectral Data”, Canadian Journal of Remote Sensing (submitted).

Snedecor G.W., and W.G. Cochran, 1967, Statistical Methods, The Iowa State University Press, Ames, Iowa, 593 pages.

Staenz, K., T. Szeredi, R.J. Brown, H. McNairn, and R. VanAcker, 1997, “Hyperspectral Information Extraction Techniques Applied to Agricultural *casi* Data for Detection of Within-Field Variations”, Proceedings of the International Symposium in the Era of Radarsat and the Nineteenth Canadian Symposium on Remote Sensing, Ottawa, Ontario, Canada, 8 pages (CD-ROM).

Staenz, K., and D.J. Williams, 1997, “Retrieval of Surface Reflectance from Hyperspectral Data Using a Look-Up Table Approach”, Canadian Journal of Remote Sensing, 23(4):354-368.

Staenz, K., T. Szeredi, and J. Schwarz, 1998, “ISDAS – A System for Processing/Analyzing Hyperspectral Data”, Canadian Journal of Remote Sensing, 24(2):99-113.

Szeredi, T., K. Staenz, and R.A. Neville, 1999, “Automatic Endmember Selection: Theory”, Remote Sensing of Environment (submitted).

Van Der Meer, 1994, ”Extraction of Mineral Absorption Features from High Spectral Resolution Data Using Non-Pararametric Geostatistical Techniques”, International Journal of Remote Sensing, 15(11):2193-2214.

Van Der Meer, F., and W. Bakker, 1997, “CCSM: Cross Correlogram Spectral Matching”, International Journal of Remote Sensing, 18(5):1197-1201.